United States
Department of
Agriculture

Agricultural
Research
Service

Agricultural
Handbook
Number XXX

Rangeland Hydrology and Soil Erosion Processes: A guide for Conservation Planning with the Rangeland Hydrology and Erosion Model (RHEM)

Draft of USDA Rangeland Hydrology and Soil Erosion Processes: A guide for Conservation Planning with the Rangeland Hydrology and Erosion Model (RHEM)   June 13, 2017

Editors: Mark Weltz and Gary Frasier

Contributors:

Mark A. Weltz, Research Leader, Rangeland Hydrologist; USDA-ARS, Reno, NV
Mariano Hernandez, Hydrologist, USDA-ARS, Tucson, AZ, Tucson, AZ
Mark A. Nearing, Research Agricultural Engineer, USDA-ARS, Tucson, AZ
Ken E. Spaeth, Rangeland Management Specialist, USDA-NRCS, Dallas, TX
Fred B. Pierson, Research Leader, USDA-ARS, Boise, ID
C. Jason Williams, Research Hydrologist, USDA-ARS, Tucson, AZ
Osama Z. Al-Hamdan, Assistant Professor, Texas A&M Kingsville, Kingsville, TX
S. Kossi, Nouwakpo, Soil Scientist, University of Nevada Reno, Reno, NV.
Gerardo Armendariz, IT Specialist, USDA-ARS, Tucson, AZ
Dave Goodrich, Research Hydraulic Engineer, USDA-ARS, Tucson, AZ
Phil Guertin, Hydrologist, University of Arizona, Tucson, AZ
Kenneth McGwire, Physical Scientist, Desert Research Institute, Reno, NV.
Jason Nesbit, IT Specialist, USDA-ARS, Reno, NV

Citation:

Abstract: Soil loss rates on rangelands are considered one of the few quantitative indicators for assessing rangeland health and conservation practice effectiveness. An erosion model to predict soil loss specific for rangeland applications is needed. Existing erosion models were developed from croplands. Hydrologic and erosion processes are different on rangelands than croplands due to much higher levels of heterogeneity in soil and plant properties and the consolidated nature of the soils. The purpose of this series of Handbooks are to improve the understanding of hydrologic processes and sources and transport mechanisms of sediment in rangeland catchments. The first Handbook Rangeland Hydrology and Soil Erosion Process provides a review of relevant rangeland hydrology literature on what is known about the impact of range management practices and field experiments conducted across the western United States. This Handbook provides the background for understanding how to use the Rangeland Hydrology and Erosion Model (RHEM) and understand it output for making informed decisions before implementing new management actions. The RHEM model is a newly conceptualized, process-based erosion prediction tool specific for rangeland application, based on fundamentals of infiltration, hydrology, plant science, hydraulics, and erosion mechanics. The model is event-based and was developed specifically from rangeland data. The erosion prediction tool estimates runoff, erosion, and sediment delivery rates and volumes at the spatial scale of the hillslope and the temporal scale of a single rainfall event. The data used to develop and validate the RHEM series of tools is contained within the USDA-ARS Agricultural, Runoff, Erosion, and Salinity database (ARES). This database contains over 2,000 rainfall simulation plots and 100 plant communities collected over the last 40 years across the western United States. These data can be used to understand ecological processes when combine with the RHEM tools to provide sound science when making critical land management decisions. The RHEM assessment tool provides information that can be combined with state and transition models and enhance Ecological Site Descriptions. The information on how to develop hydrologic sections of ESD's is contained in the 3rd Handbook. The ESD Handbook is designed to inform land managers of the benefits and consequences of changing from one ecological state to another ecological state. The RHEM assessment tool has been incorporated into the Automated Geospatial Watershed Assessment (AGWA) tool for understanding and predicting hydrologic and soil erosion processes at the watershed scale. How to estimate watershed scale hydrologic and soil erosion processes is addressed in the 4th Handbook. With these 4 Handbooks the user can understand causes and consequences of soil erosion and design management plans to prevent or correct issue of concern on rangelands.

Rangeland Hydrology and Soil Erosion Processes: A guide for Conservation Planning with the Rangeland Hydrology and Erosion Model (RHEM)

CONTENTS

Rangeland Hydrology and Erosion Model Technical Documentation

Draft of USDA Rangeland Hydrology and Soil Erosion Processes: A guide for Conservation Planning with the Rangeland Hydrology and Erosion Model (RHEM)   June 13, 2017

Contributors:

Mariano Hernandez, Hydrologist, USDA-ARS, Tucson, AZ, Tucson, AZ
Mark A. Nearing, Research Agricultural Engineer, USDA-ARS, Tucson, AZ
Mark A. Weltz, Research Leader, Rangeland Hydrologist; USDA-ARS, Reno, NV
Ken E. Spaeth, Rangeland Management Specialist, USDA-NRCS, Dallas, TX
Fred B. Pierson, Research Leader, USDA-ARS, Boise, ID
C. Jason Williams, Research Hydrologist, USDA-ARS, Tucson, AZ
Osama Z. Al-Hamdan, Assistant Professor, Texas A&M Kingsville, Kingsville, TX
S. Kossi, Nouwakpo, Soil Scientist, University of Nevada Reno, Reno, NV.
Kenneth McGwire, Physical Scientist, Desert Research Institute, Reno, NV.

Rangeland Hydrology and Erosion Model Technical Documentation

CONTENTS

Introduction

The complex interactions of variable climate, vegetation, surface soil dynamics, and human activities have major impacts on runoff and soil erosion processes on rangeland ecosystems. These processes and activities affect ecosystem function over a wide range of spatial and temporal scales (Williams et al., 2016). Nearing et al. (2004) suggested that climatic variability will increase erosion in the future in many environments. That is, future climates are expected to lead to a more vigorous hydrological cycle, including total rainfall amount and variability, and more frequent high-intensity rainfall events that drive the water erosion process (Nearing et al., 2004; Nearing et al. 2015). The consequence is often rangeland degradation, that is, a decrease in vegetation cover and∕or a change of vegetation composition with a subsequent loss of the systems productivity (UNCCD 1994). Decades of research have shown that rangelands can sustainably produce a variety of goods and services even in the face of extreme climatic events if managers respond quickly and appropriately to changes (Havstad et al., 2009). While land managers may not be able to alter variability in climate they may be able to adapt to changes in precipitation intensity, duration, and frequency and devise management practices that are more resilient and resistant to climatic impacts. Soil erosion is among the climate-related impacts that concern rangeland managers since conservation of topsoil is critical to sustained productivity in rangeland ecosystems. Soil loss rates on rangelands are regarded as one of the few quantitative indicators for assessing rangeland health and conservation practice effectiveness (Nearing et al., 2011 and Weltz et al., 2014).

The Rangeland Conservation Effects Assessment Project (CEAP) was formally initiated in 2006 to evaluate conservation effectiveness on rangelands, pastures, and grazed forests that together comprise 188 million hectares of USA nonfederal land, as well as large areas of federal

land in the western United States. Broad-scale assessments of this type need reliable modeling capabilities. Erosion prediction technology must be capable of simulating the complex interactions between vegetation characteristics, surface soil properties and hydrologic and erosion processes on rangelands (Nearing and Hairsine 2011). Al-Hamdan et al. (2012b) pointed out that better representation of the temporal dynamics of soil erodibility related to disturbed rangeland conditions (e.g., fire) is also needed to accurately estimate soil erosion on rangelands .

The goals of this Handbook is provide an exact description of the RHEM V2.3 model by providing a detailed layout of the mathematical model structure and to present the results of model applications and potential uses. The Handbook also demonstrates the gains in model performance and reliability over the former model version RHEM V1.0. The Handbook has the following sections: (1) to present the driving equations for RHEM V2.3 model; (2) to calibrate the RHEM V2.3 model using 23 rainfall-runoff-sediment yield events on a small semiarid sub-watershed within the Walnut Gulch Experimental Watershed in Arizona, and compare them against parameters estimated by the RHEM V2.3 parameter estimation equations; (3) to examine the performances improvement from RHEM V1.0 to RHEM V2.3; (4) to User Guide for implementing the model; (5) present case studies for application and interpretation of the model for planning conservation; and (6) present where data was derived to develop and validate the model.

Model Description

This section is divided into four main parts as follows. (1) presentation of fundamental hydrologic and erosion equations in RHEM V2.3, (2) an overview of the RHEM V2.3 parameter estimation equations, (3) model calibration with the Model-Independent **P**arameter **EST**imation (PEST) program, and (4) statistical analysis and results.

Fundamental hydrologic and erosion equations

    o **Overland flow model**

The hydrology component of the enhanced RHEM V2.3 model is based on the

KINEROS2 model (Smith et al., 1995). The model was implemented to simulate one-

dimensional overland flow within an equivalent plane representing a hillslope with uniform or

curvilinear slope profiles. The flow per unit width across a plane surface as a result of rainfall

can be described by the one-dimensional continuity equation (Woolhiser et al. 1990).

$$\frac{\partial h}{\partial t} + \frac{\partial q}{\partial x} = \sigma(x, t) \qquad (1)$$

where h is the flow depth at time t and the position x; x is the space coordinate along the

direction of flow; q is the volumetric water flux per unit plane width (m^2 s^{-1}); and σ (x, t) is the

rainfall excess (m s^{-1}).

$$\sigma(x, t) = r - f \qquad (2)$$

where r is the rainfall rate (m s^{-1}), and f is the infiltration rate (m s^{-1}). The following equation

represents the relationship between q and h:

$$q = \left(\frac{8gS}{f_t}\right)^{1/2} h^{3/2} \qquad (3)$$

where g is the gravity acceleration (m s^{-2}), S is the slope gradient (m m^{-1}), and f_t is the total

Darcy-Weisbach friction factor estimated using equation 18 developed by (Al-Hamdan et al.,

2013). Substituting Equations (2) and (3) in Equation (1) results in the hydrology routing equation:

$$\frac{\partial h}{\partial t} + \frac{3}{2}\left(\frac{8gS}{f_t}\right)^{1/2} h^{1/2} \frac{\partial h}{\partial x} = r - f \qquad (4)$$

In RHEM, for a single plane, the upstream boundary is assumed to be at zero depth and the downstream boundary is a continuing plane (along the direction of flow).

$$h(0, t) = 0 \qquad (5)$$

The infiltration rate is computed in KINEROS2 using the three-parameter infiltration equation (Parlange et al., 1982), in which the models of Green and Ampt (1911) and Smith and Parlange (1978) are included as two limiting cases.

$$f = K_e \left[1 + \frac{\alpha}{\exp\left(\frac{\alpha I}{C_d \triangle \theta_i}\right) - 1} \right] \qquad (6)$$

where I is the cumulative depth of the water infiltrated into the soil (m), K_e is the surface effective saturated hydraulic conductivity (m s^{-1}), C_d (m) accounts for the effect of capillary forces on moisture absorption during infiltration, and α is a scaling parameter. When $\alpha=0$, Equation 6 is reduced to the simple Green and Ampt infiltration model, and when $\alpha=1$, the equation simplifies to the Parlange model. Most soil exhibit infiltrability behavior intermediate to these two models, and KINEROS2 uses a weighting α value of 0.85 (Smith et al., 1993). The state variable for infiltrability is the initial water content, in the form of the soil saturation deficit,

$B = C_d(\theta_s - \theta_i)$, defined as the saturated moisture content minus the initial moisture content.

The saturation deficit $(\theta_s - \theta_i)$ is one parameter because θ_s is fixed from storm to storm. For

ease of estimation, the KINEROS2 input parameter for soil water is a scaled moisture content,

$S=\theta/\phi$, (ϕ is the soil porosity) which varies from 0 to 1. Thus initial soil conditions are

represented by the variable S_i ($=\theta_i/\phi$). Thus, there are two parameters, K_e, and C_d to characterize

the soil, and the variable S_i to characterize the initial condition

Overland soil erosion, deposition, and transport

The RHEM erosion model uses a dynamic sediment continuity equation to describe the

movement of suspended sediment in a concentrated flow area (Bennett, 1974).

$$\frac{\partial (Ch)}{\partial t} + \frac{\partial (Cq_r)}{\partial x} = D_{ss} + D_{cf} \qquad (7)$$

Where C is the measured sediment concentration (kg m^{-3}), q_r is the flow discharge of

concentrated flow per unit width (m^{-2} s^{-1}), D_{ss} is the splash and sheet detachment rate (kg s^{-1} m^{-2}),

and D_{cf} is the concentrated flow detachment rate (kg s^{-1} m^{-2}). For a unit wide plane, when

overland flow accumulates into a concentrated flow path, the following equation calculates the

concentrated flow discharge per unit width (q_r):

$$q_r = \frac{q}{w} \qquad (8)$$

Where w is the concentrated flow width (m) calculated by (Al-Hamdan et al., 2012a)

$$w = \frac{2.46 \, Q^{0.39}}{S^{0.4}} \qquad (9)$$

The splash and sheet detachment rate (D_{ss}) is calculated by the following equation (Wei et al.,

2009):

$$D_{ss} = K_{ss}r^{1.052}\sigma^{0.592} \qquad (10)$$

where K_{ss} is the splash and sheet erodibility, r (m s^{-1}) is the rainfall intensity and σ is rainfall

excess

(m s^{-1}).

RHEM is a hillslope scale model. As such it does not address flow in channels. It does

have the capability to estimate transport and erosion in ephemeral (rills) or semi-permanent

micro-channels on the hillslopes of up to a few cm in width and depth. Concentrated flow

detachment rate (D_{cf}) is calculated as the net detachment and deposition rate (Foster, 1982):

$$D_{cf} = \begin{bmatrix} D_c\left(1 - \dfrac{CQ}{T_c}\right), CQ \le T_c \\ \dfrac{0.5\,V_f}{Q}(T_c - CQ), CQ \ge T_c \end{bmatrix} \qquad (11)$$

where D_c is the concentrated flow detachment capacity (kg s^{-1} m^{-2}); Q is the flow discharge (m^3 s^{-1}); T_c is the sediment transport capacity (kg s^{-1}); and V_f is the soil particle fall velocity (m s^{-1})

that is calculated as a function of particle density and size (Fair and Geyer, 1954).

Sediment detachment rate from the concentrated flow is calculated by employing soil

erodibility characteristics of the site and hydraulic parameters of the flow such as flow width and

stream power. Soil detachment is assumed to start when concentrated flow starts (i.e. no

threshold concept for initiating detachment is used) (Al-Hamdan et al., 2012b).

To calculate D_c, the equation developed by Al-Hamdan et al. (2012b) is used:

$$D_c = K_\omega(\omega) \qquad (12)$$

where K_ω is the stream power erodibility factor ($s^2\ m^{-2}$) and ω is the stream power ($kg\ s^{-3}$). We implemented the empirical equation developed by Nearing et al. (1997) to calculate the transport capacity (T_c).

$$Log_{10}\left(\frac{10T_c}{w}\right) = -34.47 + 38.61 * \frac{\exp[0.845 + 0.412\log(1000\omega)]}{1 + \exp[0.845 + 0.412\log(1000\omega)]} \qquad (13)$$

Soil detachment is not considered as a selective process, so the sediment particles size distribution generated from actively eroding areas is assumed to be a function of the fraction of total sediment load represented by five particle classes based on soil texture. The transport capacity equation of Nearing et al. (1997) does not account for particle sorting. Consequently, routing of sediment by size particle is not carried out.

Several studies have documented increases in peak flows and erosion occurring on systems that have been altered by some disturbance. For example, at the plot/hillslope scale, factor increases in sediment delivery between 2- and 1000 -fold have been reported (Morris and Moses, 1987; Scott and Van Wyk, 1992; Shakesby et al., 1993; Cerdà, 1998; Pierson et al., 2002). Results from rainfall simulator experiments suggest that erosion rates are much higher in the early part of a runoff event than in the latter part of the event on forest roads (Foltz et al., 2008) and burned rangeland (Pierson et al., 2008). These rapid changes in the concentrated flow erosion rate on disturbed soils may be caused by the winnowing of fine or easily detached soil

particles during the early stages of erosive runoff, thus leaving larger or more embedded particles and/or aggregates which require greater stream power for detachment (Robichaud et al., 2010).

Because RHEM V2.3 is a dynamic model, it also has the capacity, as an option, to use equations developed by Al-Hamdan et al. (2012b) for characterizing events on recently disturbed rangelands with high concentrated flow erodibility at the onset of the event and with exponentially decreasing erodibility throughout the event due to reduction in sediment availability (winnowing of readily available sediment).

$$D_c = K_{\omega(Max)adj} \exp(\beta \, q_c)\omega \qquad (14)$$

$$q_c = \int q_r dt \qquad (15)$$

$$\omega = \gamma S q_r \qquad (16)$$

where $K_{\omega(Max)adj}$ is the maximum stream power erodibility ($s^2 \, m^{-2}$) corresponding to the decay factor $\beta = -5.53$ (m^{-2}), β is a decay coefficient representing erodibility change during an event (m^{-2}), ω is the stream power (kg s^{-3}), q_c is the cumulative flow discharge of concentrated flow per unit width (m^2), γ is the water specific weight (kg m^{-2} s^{-2}), and S is the slope gradient (m m^{-1})

RHEM Model Parameter Estimation Equations

An important aspect of RHEM with regards to application by rangeland managers is that the model is parameterized based on plant growth form types using data commonly collected in rangeland inventory and assessment efforts (e.g. rangeland health or NRI assessments).

Effective saturated hydraulic conductivity

Research has indicated that infiltration, runoff, and erosion dynamics are correlated with the presence/absence and composition of specific plant taxa and growth attributes (Davenport et al., 1998, Wainwright et al., 2000, Ludwig et al., 2005, Peters et al., 2007, Turnbull et al., 2008, Turnbull et al., 2012, Petersen et al., 2009, Pierson et al., 2010, Pierson et al., 2013, Wilcox et al., 2012 and Williams et al., 2014). Numerous studies have documented that infiltration of rainfall increases with increasing vegetative surface cover (Ludwig et al., 2005). For example, Tromble et al. (1974) evaluated infiltrability on three range sites in Arizona and found infiltrability was positively related to vegetal cover and litter biomass and negatively related to gravel cover. Meeuwig (1970) and Dortignac and Love (1961) also found infiltrability and litter cover to be positively related. Work by Spaeth et al. (1996) using data from across the western U.S. concluded that inclusion of plant species and ground cover variables in prediction equations significantly improved infiltration estimation with respect to purely physically-based prediction equations. Thompson et al. (2010) provides a detailed review of research findings on vegetation-infiltration relationships across climate and soil type gradients.

Soil texture may be used as the first estimator of K_e because texture affects the pore space available for water movement. Also, soil texture is easy to measure and often available for an area of interest. Rawls et al. (1982) developed a look-up table of K_s values for the 11 USDA soil textural classes. Bulk density is another basic soil property that is related to pore space and water movement. Rawls et al. (1998) revised the texture-based look-up table to include two porosity classes within each textural class, the geometric means of the K_s along with the 25% and 75% percentile values. The texture/porosity K_s estimates were based on a national database of measured K_s values and soil properties at 953 locations. These estimates indicate that (1) K_s is

highest for coarse-textured soils and (2) within a textural class, soils with greater porosity (lower

bulk density) have higher K_s values.

The geometric mean of K_s sorted according to the soil texture, and bulk density classes

along with the 25% and 75% percentile values are presented in Table 1. Also, reported in Table 1

is the corresponding arithmetic mean porosity ϕ (m^3 m^{-3}) and mean capillary drive C_d (mm).

Saturated hydraulic conductivity has been characterized as being lognormally distributed in

space (Nielsen et al., 1973; Smith and Goodrich, 2000), with variations of an order of magnitude

or more across relatively short distances. It is clear that representing a landscape using various

values of saturated conductivity distributed across space with a lognormal distribution is more

realistic than a single uniformly applied mean value. The RHEM model defines a range of

hydraulic conductivity values based on the 25% and 75% percentile values for each soil textural

class reported in Table 1 (Rawls et al., 1998). Then we adjusted them to account for the effects

of litter and basal cover based on the exponential model developed by Stone et al. (1992). Stone

et al. (1992) developed an exponential model to adjust the baseline saturated hydraulic

conductivity (Rawls et al., 1982) as a function of surface cover and foliar cover based on an

unpublished analysis of rainfall simulator data on desert brush dominated sites in Arizona and

Nevada. Moreover, they divided the baseline saturated hydraulic conductivity by two to account

for the effects of crusting on the effective saturated hydraulic conductivity. However, Stone et al.

(1992) did not report criteria to assess the goodness of fit of the model and the range of values of

the predictor variables. In the model developed by Stone et al. (1992), the effective saturated

hydraulic conductivity increases exponentially as ground cover and foliar cover increases, which

is consistent with the trend shown in croplands reported by Rawls et al. (1990) and Zhang et al.

(1995). Moreover, as pointed out by Zhang et al. (1995), for accurate simulation of the effects of foliar cover on infiltration and runoff, the impact of canopy height must be considered.

RHEM estimates of effective saturated hydraulic conductivity are computed as follows:

$$K_{e_i} = K_{b_i}\, e^{[p_i(\text{litter}+\text{basal})]} \qquad (17)$$

In this equation, K_{bi} is the 25% percentile saturated hydraulic conductivity for each soil textural class, i, listed in Table 1. p is defined as the natural log of the ratio of the 75% to the 25% percentile values of saturated hydraulic conductivity; litter is litter cover (%); and basal is basal area cover (%).

Hydraulic roughness coefficient

Al-Hamdan et al. (2013) developed empirical equations that predict the total measured friction factor (f_t) by regressing the total measured friction against the measured vegetation and rock cover, slope, and flow rate. The data used in their study were obtained from rangeland overland flow experiments conducted by the USDA-ARS Northwest Watershed Research Center in Boise, Idaho. Overland flow was simulated by releasing water from a flow regulator located upstream of each plot.

The data were collected from rangeland sites within the U.S. Great Basin Region, USA, with a broad range of slope gradients (5.6% to 65.8%), soil types, and vegetation cover. Many of these sites show some degree of disturbance and/or treatment, such as tree encroachment, prescribed fire, wildfire, tree mastication, and/or tree cutting. Average slope, foliar and ground cover, and micro-topography were measured for each plot (Pierson et al., 2007, 2009, 2010).

According to Al-Hamdan et al. (2013), total hydraulic friction was negatively correlated with flow discharge and the percentage of bare ground, and it was positively correlated with the presence of vegetation cover and slope. Equations that were developed from concentrated flow data have significantly different coefficients values compared to those developed from sheet flow data. The flow discharge and slope in the total friction equation improved the prediction of the total friction, and consequently improved the estimation of the proportion of the assumed soil friction to total friction. All equations derived by Al-Hamdan et al. (2013) showed that basal plant cover exerted the most influence and was the

most important effect on total friction among other measured cover attributes. RHEM computes the total Darcy-Weisbach friction (f_t) factor estimated by (Al-Hamdan et al., 2013) as follows:

$$\log(f_t) = -0.109 + 1.425 \text{ litter} + 0.442 \text{ rock} + 1.764 \text{ (basal + cryptogams)} +$$
$$2.068 \, S \qquad (18)$$

where litter is the fraction of area covered by litter to total area ($m^2 \, m^{-2}$), basal and cryptogams is the fraction of area covered by basal plants and cryptogams to total area ($m^2 \, m^{-2}$), rock is the fraction of area covered by rock to total area ($m^2 \, m^{-2}$), and S is the slope gradient ($m \, m^{-1}$).

Table 1. Estimation guides for soil hydraulic properties based on sample data (Rawls et al., 1998). The geometric mean of the K_s sorted according to soil texture and bulk density classes along with the 25% and 75% percentile.

USDA Soil Class Texture	Sand (%)	Clay (%)	Porosity ($m^3 \, m^{-3}$)	Geometric Mean K_s ($mm \, h^{-1}$)	K_s 25% percentile ($mm \, h^{-1}$)	K_s 75% Percentile ($mm \, h^{-1}$)	Mean capillary drive C_d (mm)	Sample Size
Sand	92	4	0.44	181.9	96.5	266.8	50	39
	91	4	0.39	91.4	64.0	218.5		30
Loamy Sand	82	6	0.45	123.0	83.8	195.5	70	19
	82	7	0.37	41.4	30.5	77.6		28
Sandy Loam	65	11	0.47	55.8	30.5	129.6	130	75
	68	13	0.37	12.8	5.1	31.3		112
Loam	38	23	0.47	3.9	1.6	28.4	110	44
	43	22	0.39	6.2	2.8	16.5		65
Silt Loam	18	19	0.49	14.4	7.6	37.1	200	61
	21	20	0.39	3.4	1.0	9.9		46
Sandy Clay Loam	56	26	0.44	7.7	2.0	50.5	260	20
	58	26	0.37	2.8	1.0	10.9		53
Clay Loam	29	35	0.48	4.2	2.2	13.1	260	20
	35	35	0.40	0.7	0.2	3.8		53
Silty Clay Loam	10	34	0.50	3.7	2.3	10.4	350	26
	10	32	0.43	4.9	2.3	14.0		33
Sandy Clay	51	36	0.39	0.9	0.3	2.5	300	14
Silty Clay	4	49	0.53	1.8	0.5	7.5	380	10
Clay	18	53	0.48	2.0	0.9	6.0	410	20
	26	50	0.40	1.8	0.3	6.9		21

Splash and sheet erodibility factor

The RHEM model parameterization represents erosion processes on undisturbed rangelands, as well as rangelands that show disturbances such as fire or woody plant encroachment (Nearing et al., 2011; Hernandez et al. 2013; Al-Hamdan et al. 2017; Williams et al. 2016). In RHEM, soil detachment is predicted as a combination of two erosion processes, rain splash and thin sheet flow (splash and sheet) detachment and concentrated flow detachment.

This section presents empirical equations developed by Al-Hamdan et al. (2017) using piecewise regression analysis to predict splash and sheet erodibility across a broad range of soil texture classes based on vegetation cover and surface slope gradient.

Bunch Grass:

$$\text{Log}_{10} \text{Kss} = \begin{cases} 4.154 - 2.547 * G - 0.7822 * F + 2.5535 * S & \text{if } G \leq 0.475 \\ 3.1726975 - 0.4811 * G - 0.7822 * F + 2.5535 * S & \text{if } G > 0.475 \end{cases} \quad (19)$$

Sod Grass:

$$\text{Log}_{10} \text{Kss} = \begin{cases} 4.2169 - 2.547 * G - 0.7822 * F + 2.5535 * S & \text{if } G \leq 0.475 \\ 3.2355975 - 0.4811 * G - 0.7822 * F + 2.5535 * S & \text{if } G > 0.475 \end{cases} \quad (20)$$

Shrub:

$$\text{Log}_{10} \text{Kss} = \begin{cases} 4.2587 - 2.547 * G - 0.7822 * F + 2.5535 * S & \text{if } G \leq 0.475 \\ 3.2773975 - 0.4811 * G - 0.7822 * F + 2.5535 * S & \text{if } G > 0.475 \end{cases} \quad (21)$$

Forbs:

$$\text{Log}_{10} \text{Kss} = \begin{cases} 4.1106 - 2.547 * G - 0.7822 * F + 2.5535 * S & \text{if } G \leq 0.475 \\ 3.1292975 - 0.4811 * G - 0.7822 * F + 2.5535 * S & \text{if } G > 0.475 \end{cases} \quad (22)$$

where G is the area fraction of ground cover, F is the area fraction of foliar cover, and S is the slope gradient (expressed as a fraction).

Al-Hamdan et al. (2017) reported that RHEM performed well using K_{ss} alone as long as the small concentrated flow paths on the hillslope work primarily as the transport mechanism for

the splash and sheet-generated sediments. It is recommended to use the K_{ss} equation that represents the dominant vegetation community in the site to be evaluated. However, if the site does not have a dominant vegetation form or more details are needed, then weight averaging between equations (19) through (22) based on the percentage of life form can be used.

Concentrated flow erodibility coefficients for hillslope micro-channels

The parameterization of K_ω is needed only in the special case of abrupt disturbance with steep slope gradients (>20%) and soil with high silt content. In RHEM, the default value for K_ω was set as 7.7×10^{-6} (s^2 m^{-2}) based on rainfall simulator studies carried out in Walnut Gulch Experimental Watershed in Tombstone Arizona and model calibration. This small value of concentrated flow erodibility is typical for undisturbed rangeland (Al-Hamdan et al., 2017). Moreover, Al-Hamdan et al. (2012b) developed an empirical equation to calculate K_ω for a broad range of undisturbed rangeland sites and tree encroached sites.

$$\log_{10}(K_\omega) = -4.14 - 1.28\text{litter} - 0.98\text{rock} - 15.16\text{clay} + 7.09\text{silt} \qquad (23)$$

The model also has the capacity, as an option, to use equations developed by Al-Hamdan et al. (2012b) for predicting maximum erodibility for a wide range of burned rangeland sites including burned tree encroached sites.

$$\log_{10}\left(K_{\omega(max)adj}\right)$$
$$= -3.28 - 1.77\text{litter} - 1.26\text{rock} - 2.46(\text{basal} + \text{crypto}) + 3.53\text{silt} \qquad (24)$$

$$\log_{10}\left(K_{\omega(max)adj}\right)$$
$$= -3.64 - 1.97(\text{litter} + \text{basal} + \text{crypto}) - 1.85\text{rock} - 4.99\text{clay}$$
$$+ 6.0\text{silt} \qquad (25)$$

where litter, basal, and crypto are the fraction of area covered by litter, basal, and cryptogam to total area ($m^2\,m^{-2}$), rock is the fraction of area covered by rock to the total area ($m^2\,m^{-2}$), and clay and silt fraction.

PEST model parameterization

This study employs PEST software (Doherty, 1994) to calibrate RHEM parameters and evaluate model performance for the 23 rainfall-runoff-erosion events at Lucky Hills 106 (LH106). The parameter calibration process included two approaches: first, the overland flow related parameters were calibrated (effective saturated hydraulic conductivity, total friction factor, and capillary drive). The parameters slope gradient, coefficient of variation for K_e, and Interception were held constant during the calibration. A detailed description of the overland flow parameters can be found in Smith et al. (1995); second, the calibration of the splash-and-sheet soil erodibility coefficient was achieved by keeping constant the optimized overland flow parameters.

Statistical analysis

Nash-Sutcliffe Efficiency (NSE) (Nash and Sutcliffe, 1970) between observed and calculated cumulative flows was calculated for each single event at LH106 as follows:

$$\text{NSE} = 1 - \frac{\sum_{t=1}^{T}(O_t - M_t)^2}{\sum_{t=1}^{T}(O_t - \overline{O})^2} \qquad (26)$$

where O_t, $\overline{O}$ and M_t are observed cumulative flows at time step t, average cumulative value, and modeled cumulative flows at time step t, respectively. T is the total number of time steps in the simulation for each rainfall event.

Moreover, percent bias (PBIAS) (Gupta et al., 1999) and the RMSE-observations standard deviation ratio (RSR) (Moriasi et. al., 2007) were calculated to evaluate the overall

performance of the model for runoff volume, peak runoff, and sediment yield estimates from the 23 events at LH106.

PBIAS was calculated by

$$PBIAS = \frac{\sum_{i=1}^{N}(O_i - M_i) * 100}{\sum_{i=1}^{N} O_i} \qquad (27)$$

RSR was calculated by

$$RSR = \frac{\sqrt{\sum_{i=1}^{N}(O_i - M_i)^2}}{\sqrt{\sum_{i=1}^{N}(O_i - \overline{O})^2}} \qquad (28)$$

where O_i is the observed value of event i; M_i is the model generated value for the corresponding event i; $\overline{O}$ is the average of the observed values, and N is the total number of events at LH106.

Study Area and NRI database – Model performance and capabilities

o Lucky Hills 106 watershed

The data used for the calibration and evaluation of the model were obtained from the USDA-ARS Southwest Watershed Research Center's Lucky Hills experimental site, located in the Walnut Gulch Experimental Watershed (WGEW). The semiarid WGEW is located in southeastern Arizona (31º 43'N, 110º 41'W) and surrounds the town of Tombstone, Arizona (Figure. 1). It has a mean annual temperature of 17.7ºC and a mean annual precipitation of 350 mm, the majority of which is a result of high-intensity convective thunderstorms in the summer monsoon season (Keefer et al., 2015).
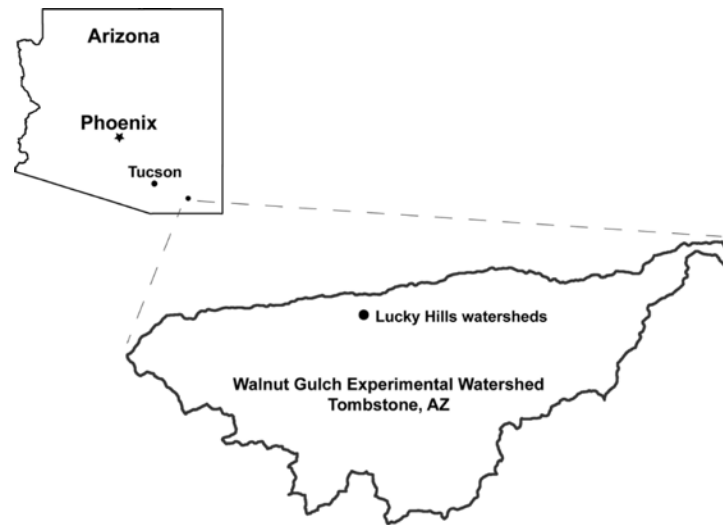
Figure 1. Location of the Lucky Hills subwatershed study area within the Walnut Gulch Experimental Watershed.

The LH106 subwatershed has an area of 0.367 hectares. The LH106 subwatershed presents an excellent location for this study because of the availability of rainfall, runoff, Time Domain Reflectometry (TDR) sensors placed at each rain gauge for estimating gravimetric soil moisture, and sediment time-series data required for model calibration at the hillslope scale. LH106 also is appropriate because it is not channelized and acts more as a large hillslope rather than a watershed with significant contribution of channel sediment (Nearing et al., 2007; Nichols et al., 2012). The slope length for the subwatershed is 65.3 m. At this scale, rainfall amount and intensity, vegetative foliar cover, ground surface cover, and micro-topography (and their spatial variability) largely determine overland flow and soil erosion processes (Lane et al., 1997). Rainfall is recorded at Rain Gauge 83 with a temporal resolution of 1 min (Figure. 2). A 1m x 1m DEM was prepared based on LIDAR survey and used to relate to micro-topography characteristics.
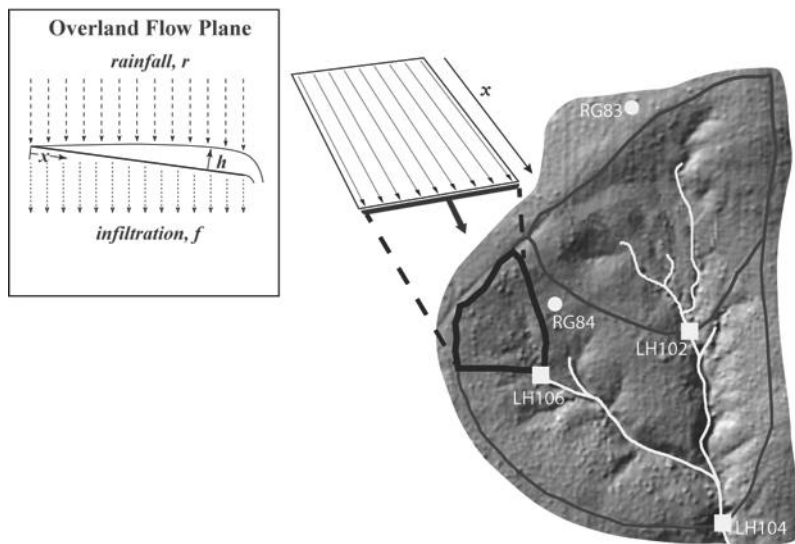
Figure 2. Lucky Hills 106 and its representation as overland flow plane in the RHEM model.

The vegetation is comprised mostly of shrubs on an 8% slope gradient. Dominant shrubs include Creosote (Larrea tridentata (Sessé and Moc. ex DC.) Coville) and Whitethorn (Acacia constricta Benth.). Foliar and ground cover information is given in Table 2. The soil is a Lucky Hills-McNeal sandy loam complex with approximately 52% sand, 26% silt, and 22% clay on a Limy Uplands (12-16"p.z.) ecological site. Rainfall and runoff data have been collected at Lucky Hills since 1963, when rain gauge 83 and weirs LH 104 and 102 were installed (Figure. 2). Rain gauge 84 was added in 1964, when an H-flume was installed on LH106 in 1965 (Figure. 2), to collect suspended sediment samples in addition to the coarse load deposited in the flume during each event (Simanton et al., 1993). Since the instrumentation was installed in the early 1960's, rainfall and runoff data have been collected with only short interruptions for upgrading equipment, which occurred during the winter (Renard et al., 1980). Sediment data are prone to periodic sampling errors, so sediment data are not available for many events for which rainfall and runoff data are available (Nearing et al., 2007).

Table 2. Summary of the ground surface and foliar cover for Lucky Hills 106 subwatershed.

Cover			
Ground Surface	**(%)**	**Foliar**	**(%)**
Basal	3	Bunch Grass	1
Rock	45	Forbs/Annual Grasses	2
Litter	10	Shrub	35
Cryptogams	0	Sod Grass	0
Total	**58**	**Total**	**38**

Twenty-three time-intensity pairs collected between 2005 and 2010 from Rain Gauge 83 as an input into the RHEM model to assess the hydrologic and erosion response of LH106 (Figure. 2). Summary descriptive statistics of rainfall, observed runoff volume, observed peak runoff, and observed sediment yield are presented in Table 3.

Next, ground surface cover, foliar cover, basal area, cryptogams cover, litter cover, rock fragment cover, and slope gradient percent were estimated for the 124 NRI points. Figures 3, 4, and 5 present the distributions for ground surface cover, foliar cover, and slope gradient grouped by annual rainfall amounts. For purposes of RHEM application, ground cover is the cover of the soil surface that essentially is in contact with the soil, as opposed to foliar cover, which is cover above the ground surface and provided by plants. Ground cover may be present in the form of plant litter, rock fragments, cryptogams, and plant bases/stems. A comprehensive review of the NRI inventory sampling strategy is presented in Goebel (1998). A review of new proposed NRI protocols on non-federal rangelands is presented in the National Resources Inventory Handbook

of Instructions for Rangeland Field Study Data Collection (USDA 2005), and a summary of NRI

results on rangeland is presented in Herrick et al. (2010).

Table 3. Summary descriptive statistics of the 23 events at Lucky Hills 106 and Rain Gauge 83.

	Mean	Min	Max	Std
Rainfall Volume (mm)	21.86	8.64	46.35	12.08
Runoff Volume (mm)	7.63	2.10	22.82	6.06
Peak Runoff Rate (mm h^{-1})	38.34	11.92	106.56	24.01
Sediment Yield (t ha^{-1})	0.23	0.03	0.94	0.23

Model performance with RHEM parameter estimation equations

Total friction factor (f_t), effective saturated hydraulic conductivity (K_e), splash and sheet

erodibility coefficient (K_{ss}), and concentrated flow erodibility coefficient ($K_\square$) were estimated

with the RHEM V2.3 empirical equations for LH106 (Table 4). We calculated $K_\square$ (4.37×10^{-6} (s^2

m^{-2})) and compared to the default value (7.74×10^{-6} (s^2 m^{-2})). The values are within the same

order of magnitude and the difference did not affect the output of the simulation results.

Consequently, we kept the default value for this study.

The model performance based on the PBIAS and RSR goodness of fit criteria for runoff

volume, peak runoff, and sediment yield at LH106 is shown in Table 5. Based on the model

performance criteria reported by Moriasi et al. (2007), model performance based on the RSR

criterion can be evaluated as "very good" if $0 \leq RSR \leq 0.5$, "good" if $0.50 < RSR \leq 0.60$,

"satisfactory" if $0.60 < RSR \leq 0.70$; and "unsatisfactory" if $RSR > 0.70$. Therefore, these

rankings suggest that RHEM performance can be

Table 4. RHEM parameter values estimated using the empirical equations.

Parameters	Symbol	Units	Value
Total friction factor	f_t	dimensionless	5.50
Effective saturated hydraulic conductivity	K_e	(mm h^{-1})	7.29
Splash and sheet erodibility coefficient	K_{ss}	(kg m$^{-3.644}$ s$^{0.644}$)	2661.22
Concentrated flow erodibility coefficient	$K_\square$	(s^2 m^{-2})	7.74x10^{-6}

evaluated as "very good" for runoff volume, "good" for peak runoff and "satisfactory" for sediment yield. However, based on Moriasi et al., (2007) PBIAS criterion, the RHEM performance can be evaluated for runoff volume and peak runoff as "very good' if PBIAS < $\pm$10, "good" if $\pm$10 $\leq$ PBIAS $\leq$ $\pm$15, and "satisfactory if $\pm$15 $\leq$ PBIAS $\leq$ $\pm$25, and for sediment yield can be evaluated as "good" if $\pm$15 $\leq$ PBIAS $\leq$ $\pm$30. These criteria suggest that RHEM can be evaluated as 'very good' for runoff volume, "satisfactory" for peak runoff, and "good" for sediment yield.

Table 5. Model performance statistics for Lucky Hills 106.

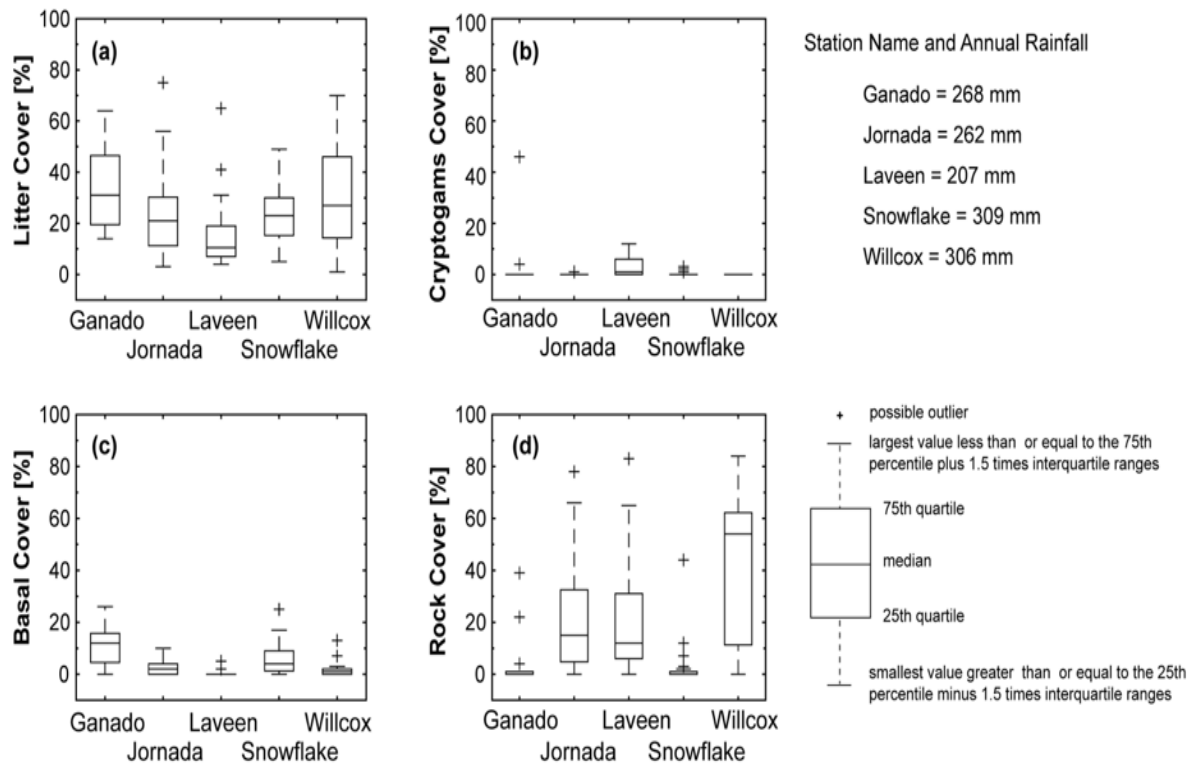| Evaluation criteria	Runoff Volume	Peak Runoff	Sediment Yield
RSR (dimensionless)	0.48	0.57	0.70
PBIAS (%)	2	21	-22

Figure 3. Distributions of ground surface cover grouped by the five weather stations. (a) Litter cover, (b) Cryptogams, (c) Basal area, and (d) Rock cover.

Positive PBIAS values indicate model underestimation bias, and negative values indicate overestimation bias (Gupta et al., 1999). It is apparent from Figure 6(a) that the model performance for runoff volume prediction is poor with small events and improves with large events, which is common for models (Nearing, 2000). Figure 6(b) shows strong under prediction of peak runoff among 14 runoff events, whereas sediment yield is in general over predicted for the small events in Figure 6(c). Hills 106: (a) Runoff volume, (b) Peak runoff and (c) Sediment yield. The parameters for these simulations were based on the RHEM V2.3 parameter estimation equations.

In the desert southwest and central plains rangeland vegetation has developed the ability to utilize rainfall from very small rainfall events (≤ 5mm). Plant communities in these area have

developed mechanism to absorb this water directly from the leaf and maintain productivity (Sala

et al., 1981). This ability is an adaptive mechanism to uncertainty in precipitation in these

droughty environments. Rainfall intensity is also key to understanding infiltration, runoff, and

soil erosion processes. Small rainfall events result in small and dense patches of vegetation

benefiting from runoff from the bare interspaces over large more spatial separated patches.

Large rainfall events benefits the larger patches in enhance runoff capture (e.g. increased soil

water) over the dense vegetation patches (Maglliano et al., 2015).
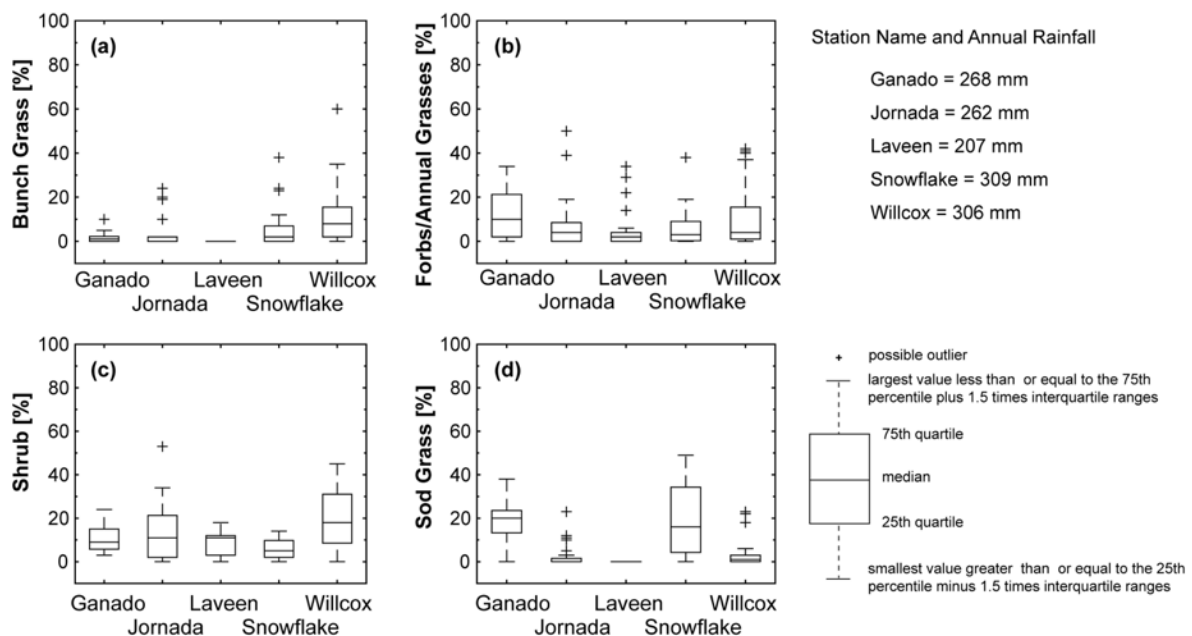
Figure 4. Distributions foliar cover grouped by the five weather stations. (a) Bunch grass, (b) Forbs/Annual grasses, (c) Shrub, and (d) Sod grasses.

Overall the interaction between the size, density, and connectivity of the bare interspace upslope

of the vegetation patch, distance upslope, slope, and rainfall intensity are the most relevant

controlling factors of how effective precipitation is in enhancing annual net primary productivity

of the vegetation patch and thus soil erosion processes (Urgeghe et al., 2010, Urgeghe et al.,

2015).

In rangelands it is the rare precipitation event (e.g., return period greater than 10 years) which may trigger a nick-point along the hillslope that can degrade the sites stability and hydrologic function by allowing water to concentrate and accelerate soil loss in concentrated flow channels and/or rills (Weltz et al., 2014). As rangelands are not tilled these flow channels and rills persist and can act to rapidly convey raindrop splash detached sediments down the hillslope in future runoff events (Wilcox et al, 1994; Davenport et al., 1998; Urgeghe et al., 2010).
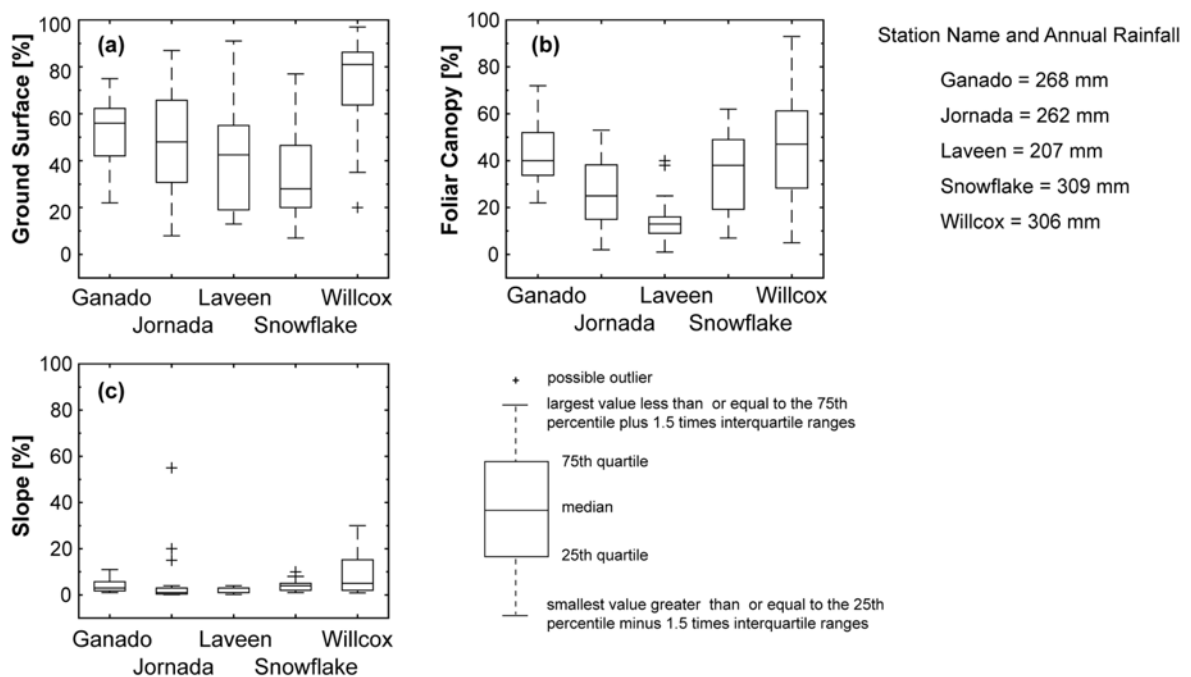
Figure 5. Distributions of total ground surface cover and foliar cover grouped by the five weather stations, and slope gradient of each NRI points classified based on the weather station's radius of influence.

Protected vegetated surfaces between flow channels and rills are safe sites, resulting in minor runoff and low sediment yield from these areas (Davenport et al., 1998; Wilcox et al., 2003; Puigdefábregas 2005; Ravi et al., 2010, Urgeghe et al., 2015). The same landscape with uniform soil disturbance and distribution of vegetation may experience significantly more runoff and soil

loss from a similar runoff event due to increased connectivity of bare soils and formation of well-organized concentrated flow paths.
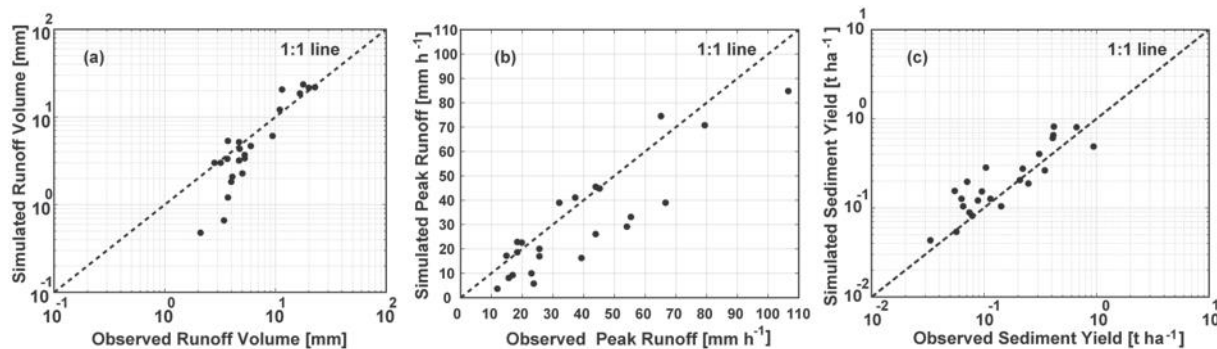

Figure 6. Comparison between observed and simulated results for each rainfall-runoff event at Lucky Lucky Hills 106: (a) Runoff volume, (b) Peak runoff and (c) Sediment yield. The parameters for these simulations were based on the RHEM V2.3 parameter estimation equations.

The RHEM V2.3 model did a good job at predicting soil erosion from the higher runoff events in comparison to RHEM V1.0. It is these high runoff and corresponding soil loss events which have the greatest impact on long-term sustainability of rangeland. RHEM V2.3 has the ability to address both undisturbed soils and disturbed soils which is required if land managers are going to make informed decision on how to alter current practices to enhance sustainability of rangelands. Based on the criteria for assessing goodness of fit of the model reported in Table 5 and the 1:1 line in Figure 6, it is reasonable to conclude that RHEM V2.3 worked reasonable well for the data from Lucky Hills.

Model calibration

The calibration process was carried out using PEST; therefore, each calibrated parameter had a different value for different rainfall events on LH106. For most events, parameters were calibrated within eight iterations, with a maximum number of 15 iterations. NSE for cumulative runoff volume ranges from 0.85 to 0.99 with a mean of 0.96, as there are ten runoff data points

and three calibrated parameters per event in the hydrology component of RHEM. The RHEM calibration produced the following average values of overland flow parameters: Total friction factor f_t =3.10 (dimensionless), K_e = 6.26 (mm h^{-1}), and net capillary drive C_d = 90 (mm). The calculated parameters by the parameter estimation equations were as follows: Total friction factor f_t = 5.50 (dimensionless) and K_e=7.29 (mm h^{-1}). The calibrated net capillary drive C_d value (90 mm) was smaller than the recommended in the KINEROS2 manual (127 mm) and reported by Rawls et al. (1982) for a sandy loam soil texture class.

The calibration of K_{ss} for each soil erosion event using PEST was achieved as follows. Total friction factor, effective saturated hydraulic conductivity, capillary drive and $K_{\Box}$ remained fixed for every calibration run. For most events K_{ss} was calibrated within three or five iterations. NSE for cumulative soil loss ranges from 0.81 to 0.96 with a mean of 0.90. The mean calibrated K_{ss} was 2089 (m^2 s^{-2}), which is lower than the value estimated by the equations proposed by Al-Hamdan et al. (2017) as reported in Table 4. The min, max, and average values for the calibrated parameters are presented in Table 6.

Table 6. **Minimum, maximum, and average values for the calibrated parameters.**

Parameter	Min	Max	Average
f_t (dimensionless)	0.96	19.62	3.10
K_e (mm h^{-1})	1.3	12.23	6.26
C_d (mm)	70	110	90
K_{ss} (m^2 s^{-2})	800	6240	2089

Performance improvement from RHEM V1.0 to RHEM V2.3

The improvement made in model efficiency for the Lucky Hills site was 60% in comparison with the previous model version RHEM V1.0, especially with respect to low sediment yield simulation as shown in Figure 7.

The system of parameter estimation equations for RHEM V1.0 were developed by Nearing et al. (2011), they used the WEPP-IRWET rangeland dataset that contains measurements of simulated rainfall, runoff, and sediment discharge and soil and plant properties on 204 plots from 49 rangeland sites distributed across 15 western states. In all studies, the rotating-boom rainfall simulator (Swanson, 1965) was used to simulate rainfall for 30 minutes at about 60 mm/hr. intensity.

Al-Hamdan et al. (2017) used the same WEPP-IRWET rangeland dataset for developing the new erodibility parameter equations in RHEM V2.3, but also used data for validation from independent rainfall simulation experiments conducted by the USDA-ARS Northwest Watershed Research Center, Boise, Idaho (Pierson et al., 2007, 2009, 2010, 2013; Moffet et al., 2007; Williams et al., 2014). These experiments were conducted using a Colorado State University type rainfall simulator (Holland, 1969) consisting of multiple stationary sprinkles elevated 3.05 m above the ground surface (Pierson et al., 2007, 2009, 2010, 2013).

As a comparison, we followed the procedure outlined in Nearing et al. (2011) for estimating RHEM V1.0 parameter values for LH106. The computed effective saturated hydraulic conductivity and the splash and sheet erodibility coefficient are as follows: $K_e = 4.76$ mm hr^{-1} and $K_{ss} = 1096$ (kg m$^{-3.644}$ s$^{0.644}$), respectively. The RHEM V2.3 effective saturated hydraulic conductivity value is 1.5 times greater than the RHEM V1.0; however, the RHEM V1.0 K_{ss} value is 2.5 smaller than the RHEM V2.3: $K_{ss} = 2661$ (kg m$^{-3.644}$ s$^{0.644}$).

Al-Hamdan et al. (2017) employed piecewise (segmented) regression analysis where two continuous relationships between the log-transformed erodibility and the independent variables were fitted to improve the linear relationship. The piecewise regression analysis revealed that the best two-piece regression occurs when the ground cover of 0.475 is the break point (see Eqs.19-22). That is, the value of 0.475 is in agreement with several studies which concluded that the erosion to runoff ratio (erodibility) increases substantially when bare ground exceeds 50% (e.g. Al-Hamdan et al., 2013; Pierson et al., 2013, Weltz et al., 1998).

The reasonable performance of the RHEM V2.3 model with the new parameterization schemes shown in Figure 7 indicates that using K_{ss} alone, as the indicator of erodibility factor in RHEM, works reasonable well for this case.

Model application using NRI data

This section reports a case study of application of the model on a number of sites to assess the simulated effects of ground cover on total friction factor (f_t), effective saturated hydraulic conductivity (K_e), and splash and sheet erodibility factor (K_{ss}) estimated using the parameter estimation equations, as well as the effect of foliar cover and ground cover on sediment yield.

To investigate these effects, we applied the model to the 124 NRI points. The RHEM V2.3 model was run for a 300-year synthetic rainfall sequence generated by CLIGEN V5.3 (Nicks et al., 1995) based on the statistics of historic rainfall at each climate station. This is the default setup for running RHEM within the user interface. The associations between ground cover and $\log_{10}$ (f_t), K_e, and K_{ss} are shown in Figure 8. They provide a basis for evaluating the behavior of the parameter estimation equations. That is, $\log_{10}$ (f_t) increased with increasing ground cover as shown in Figure 8(a), the strong positive correlation coefficient (r= 0.79, p < 0.05), suggesting that the parameter estimation equation to predict total friction roughness was

not affected by outliers or small departures from model assumptions. For example, a slope

gradient of 55% was reported in one NRI plot as shown in Figure 5(c). Similarly, we expected

that K_e would increase with increased litter cover and basal area cover as shown in Figure 8(b).

Although the spread of K_e around 80% ground cover, with the moderate correlation coefficient

(r=0.46, $p < 0.05$), suggests that the parameter estimation equation for predicting K_e for a sandy

loam soil texture class was not affected by small departures from model assumptions.

The rate of rapidly increasing K_{ss} starts at about 45% ground cover; this threshold value

is consistent with several studies that concluded that ground cover should be maintained above a

critical threshold of ~50-60% to protect the soil surface adequately Gifford's (1985) and Weltz et

al. (1998). A strong negative Spearman correlation coefficient (rho = -0.71, $p < 0.05$) and a fitted

decaying exponential model ($R^2 = 0.82$, $p < 0.05$) to the data shown in Figure 8(c) confirms the

expected decreasing monotonic trend between ground cover and K_{ss}, and the NRI point with

55% slope gradient did not appear to cause an adverse effect on the correlation coefficient and

fitted decaying exponential model.

Given that vegetation contributes much to the hydrologic and hydraulic properties of the

surface, it is logical to account for the vegetation in the surface runoff process. To investigate the

influence of litter and basal cover on percent runoff, defined as the ratio of runoff to

precipitation, we found a strong negative linear correlation (r = - 0.70, $p < 0.05$) with litter as

depicted in Figure 9(a). Furthermore, two distinct patterns of percent runoff emerged as a

function of annual rainfall amount observed at the Ganado and Willcox weather stations. That is,

both weather stations' area of influence had similar average amounts of litter cover percent

(Ganado: mean=34% and Willcox: mean=31%), but distinct annual rainfall regimes (Ganado:

268 mm and Willcox: 306 mm). Furthermore, the Ganado's area of influence is characterized by

sod grasses (mean=19%) and forb/annual grasses (mean=12%), and the Willcox's area is

characterized by a combination of shrub (mean=19 %), bunch grasses (12%), and forb/annual

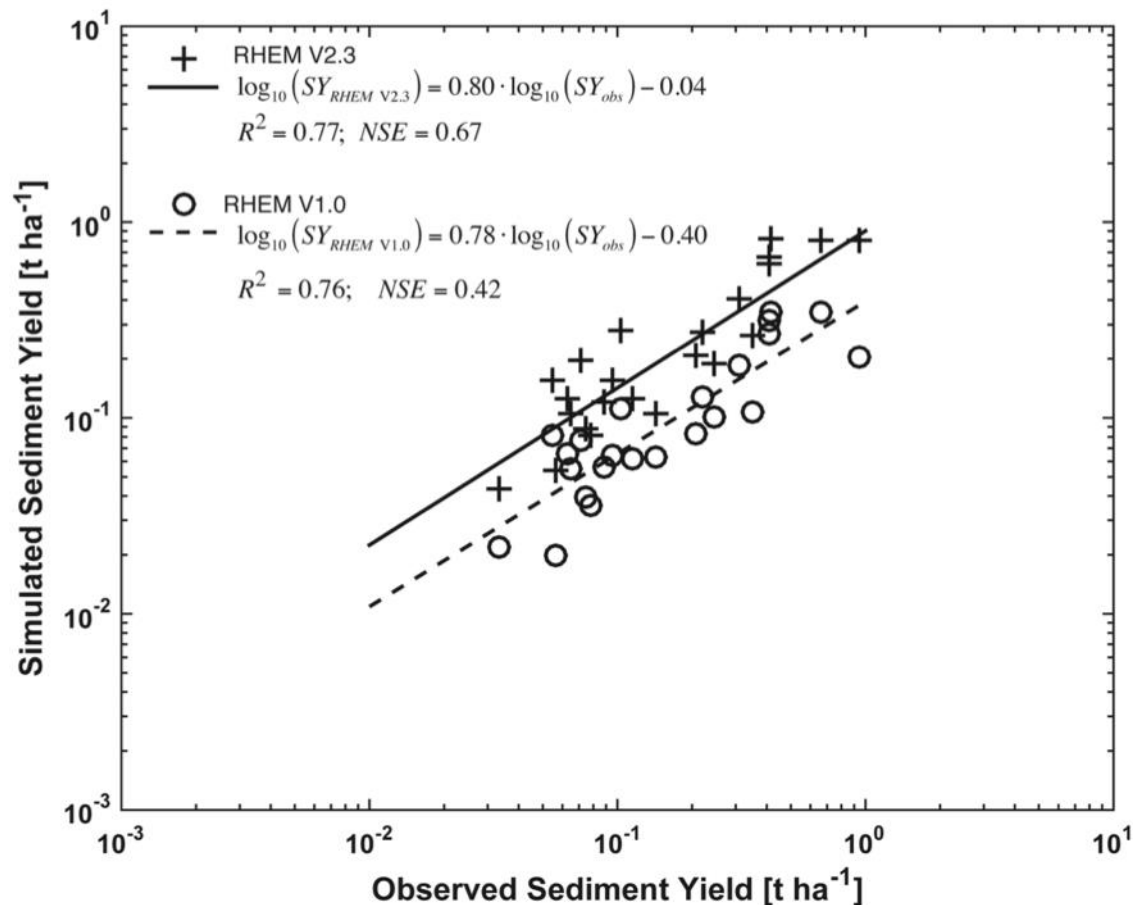grasses (mean=11%). The Laveen weather station has the lowest annual rainfall amount

Figure 7. Performance improvement on the 23 LH106 sediment yield events by both RHEM V2.3 and RHEM V1.0 models according to the NSE criterion.

 (207mm) and the lowest litter cover percent (16%), and it is mainly shrub-forb/annual grasses-

dominated (mean=9% and mean=6%, respectively).

To investigate the influence of basal cover on percent runoff, we found a moderate

negative relationship depicted in Figure 9(b). Although no patterns emerged in this relation, the

model was able to capture the influence of basal dynamics by showing a negative trend.

Transport capacity increases as flow rate and slope steepness increase. The parameter estimation equations for calculating concentrated flow width, hydraulic roughness, and splash and sheet erodibility depend on the geometry of the upland area as described by the surface slope steepness. Figure 10 shows the graph of annual sediment yield versus slope steepness for the 124 NRI points.
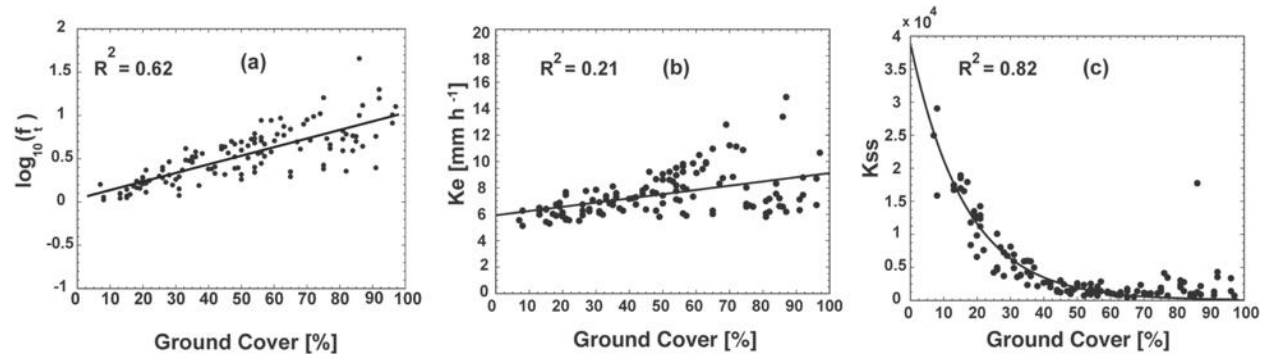

Figure 8. The association between ground cover and total friction factor (f_t), effective saturated hydraulic conductivity (K_e) and splash and sheet erodibility coefficient (K_{ss}). (a) strong positive linear correlation between ground cover and $\log_{10}(f_t)$, (b) moderate linear correlation between ground cover and K_e, and (c) strong Spearman rank correlation coefficient between ground cover and K_{ss}.

It can be seen that they are strongly correlated ($R^2=0.65$; $p<0.001$) with a large variability around the 1% and 3% slope gradient interval, 60% of the points falls within this percent interval. The variability represented by the coefficient of variation (CV) in slope gradient, litter, rock and annual sediment yield of the five rainfall regimes is reported in Table 7. The variability in rock cover on the Ganado, Jornada Experimental Range, Laveen and Snowflake and slope gradient on the Jornada Experimental Range contribute to some extent to the large variability in annual
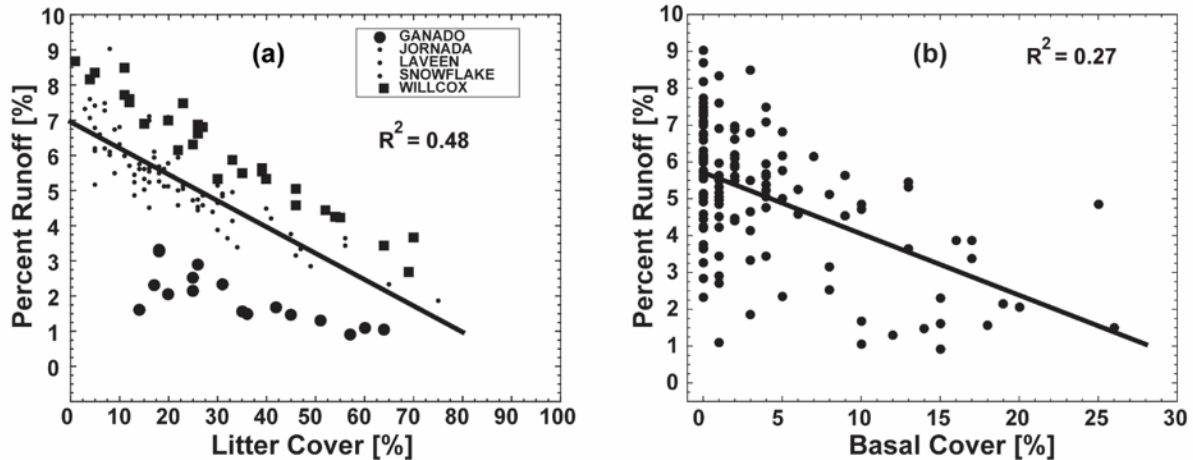
Figure 9. Runoff as a percent of precipitation showing the negative relationship with (a) litter cover percent and (b) basal cover percent.

sediment yield. Moreover, a coefficient of variation less than 1 is considered to be low-variance, consequently, the variability in simulated sediment yield was less affected by the dispersion in litter cover, and slope gradient, except for the Jornada Experimental Range.

We estimated the correlation coefficient to measure the strength of association between average annual sediment yield and the variables foliar cover and ground cover, and grouped by weather stations. Since the variability in sediment yield for each precipitation regime was large, sediment yield was normalized to fit a single equation to the sediment yield, foliar cover and ground cover data from each precipitation regime. The mean slope gradient percent of NRI points within each precipitation regime represented by the five weather stations shown in Table 7 was selected for the normalization. The results are shown in Figure 11.

The strength of the association between average annual sediment yield and foliar and ground cover is moderate to strong; the correlation coefficient varied from -0.39 to -0.81 and -0.72 to -0.95 for foliar and ground cover, respectively. When shrub is the dominant plant form, the relationship between sediment yield and foliar cover is the strongest as shown in Figs. 11(c and

i). Conversely, the weakest relationship between sediment yield and foliar cover appears to be when sod or forbs are the dominant plant forms as indicated in Figs. 11(a, e, and g). The area covered by the Ganado weather station has the fewest number of NRI points (n=17) and is dominated by forbs/annual grasses and sod grasses. The low number of NRI points and the high variability in these grasses, as shown in Figs. 4(b and d), can be attributed to the fact that only15% of the variability between the annual sediment yield and foliar cover can be accounted for. When litter and rock cover are the most dominant variables, the association between average annual sediment yield and ground cover is very strong, as indicated in Figs. 11(b, d, f, h, and j). These results suggest that low yearly sediment yield, in general, is not well described by foliar cover. We found that the association is stronger with ground cover than with foliar cover, which is expected (e.g., Nearing et al., 2005). The results suggest that ground cover, in general, is more highly associated with yearly sediment yield than is foliar cover.
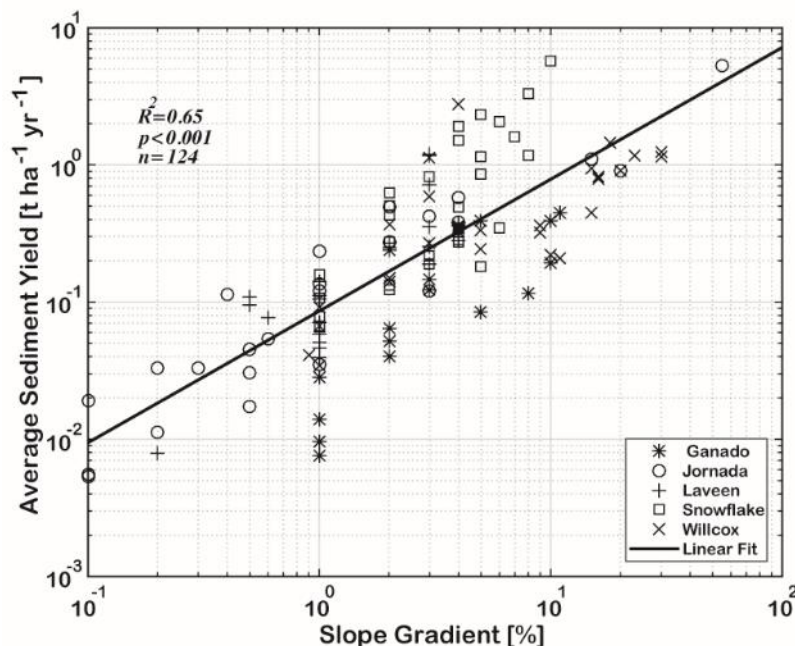

Figure 10. **Relationship between average annual sediment yield and slope gradient for the 124 NRI points affected by 5 precipitation regimes.**

Table 7. Variation of mean and CV in slope steepness, litter, rock and annual sediment yield for the 124 NRI points.

Weather Station	n		Slope		Litter		Rock		Annual Sediment Yield	
			Mean (%)	CV	Mean (%)	CV	Mean (%)	CV	Mean (t ha^{-1})	CV
Ganado	17	268	4.18	0.83	34.35	0.47	3.94	2.66	0.16	0.95
Jornada Exp Range	25	262	4.64	2.48	23.96	0.73	22.64	1.06	0.42	2.51
Laveen	22	207	1.81	0.67	16.00	0.91	21.18	1.01	0.27	1.24
Snowflake	31	309	3.74	0.63	24.00	0.49	2.35	3.45	0.88	1.36
Willcox	29	306	9.10	0.96	31.45	0.62	39.97	0.73	0.59	1.01

Conclusions

In this article, we presented an improved version of the RHEM model. This model was developed to fill the need for a process-based rangeland erosion model that can function as a practical tool for quantifying runoff and erosion rates specific to western U.S. rangelands to provide reasonable runoff and soil loss prediction capacity for rangeland management and research.

The capability of RHEM V2.3 for simulating flow and soil erosion was tested on a small watershed in Arizona and on 124 NRI plots placed in Arizona and New Mexico. In particular, we were interested in evaluating the parameter estimation equations of the RHEM V1.0 and RHEM V2.3 models for predicting

total friction factor (f_t), effective saturated hydraulic conductivity (K_e), splash and sheet erodibility coefficient (K_{ss}), and concentrated flow erodibility coefficient ($K_\square$).

The improvement made in model efficiency is significant in comparison with the original version RHEM V1.0 when the new equations for estimating K_{ss} are used, especially with respect to low-sediment yield simulation. In developing RHEM, we were aware that the model would evolve in the future to further improve its reliability as progress was made in conducting new rainfall simulator experiments and exploring new model structure for defining parameter estimation equations. The evaluation of the new erodibility equations conducted by Al-Hamdan et al. (2017) showed the ability of the RHEM V2.3 model to predict erosion at the plot scale with a satisfactory range of error. The test that we conducted here of the RHEM V2.3 model at the hillslope scale showed that, compared to the RHEM V1.0 model, its results for this site were statistically robust.

The parameter values calculated with the parameter estimation equations fell within the lowest and highest calibrated values of each parameter. The ability of the parameter estimation equations to adequately produce parameter values for the application of RHEM V2.3 on a small watershed suggest that the model is suited for small sub-watersheds, provided that gully erosion and side wall sloughing are not the main active soil erosion process in the watershed.

The analysis of the 124 NRI points in Arizona and New Mexico suggests that the parameter estimation equations conveyed coherent information to the model. That is, moderate and strong negative correlation coefficients between ground cover percent and total friction factor, effective hydraulic conductivity, and splash and sheet erodibility coefficient were achieved. Likewise, moderate and strong negative correlation coefficients were found between litter cover and basal cover percent and percent runoff. Similarly, moderate and strong negative correlation

coefficients were found between foliar cover and ground cover and sediment yield. In general, the model results are more sensitive to ground cover than to foliar cover, which is a product of the structure of the parameter estimation equations. This is consistent with our understanding of the basic processes of soil erosion, largely because of shear stress partitioning (Foster, 1982), and of most soil erosion models (Nearing et al., 2005).

Evaluation of the model predictions undertaken in this study demonstrates that RHEM V2.3 produces results of satisfactory quality when simulating large flow and soil erosion events, but a greater degree of uncertainty is associated with predictions of small runoff and soil erosion events. The reasonable performance of the model with the new parameterization equations indicates that using K_{ss} alone works reasonable well as long as concentrated flow paths function only for transport of the splash and sheet-generated sediment, as opposed to functioning also as significant sediment source. Our test of the model was conducted on an undisturbed hillslope with a mild slope gradient (8%); therefore, the concentrated flow erodibility was negligible and the estimation of the concentrated flow erodibility coefficient (K_ω) was not needed. In order for concentrated flow paths on rangelands to generate sediment detachment they need to have high erodibility values (i.e., high availability of erodible sediments) and high erosivity (i.e., stream power which increases with slope steepness). Further research needs to be carried out at the hillslope scale to study the special case of abrupt disturbance, such as post-fire, with steep slope gradients whereby both K_ω and K_{ss} erodibility parameters might be needed.
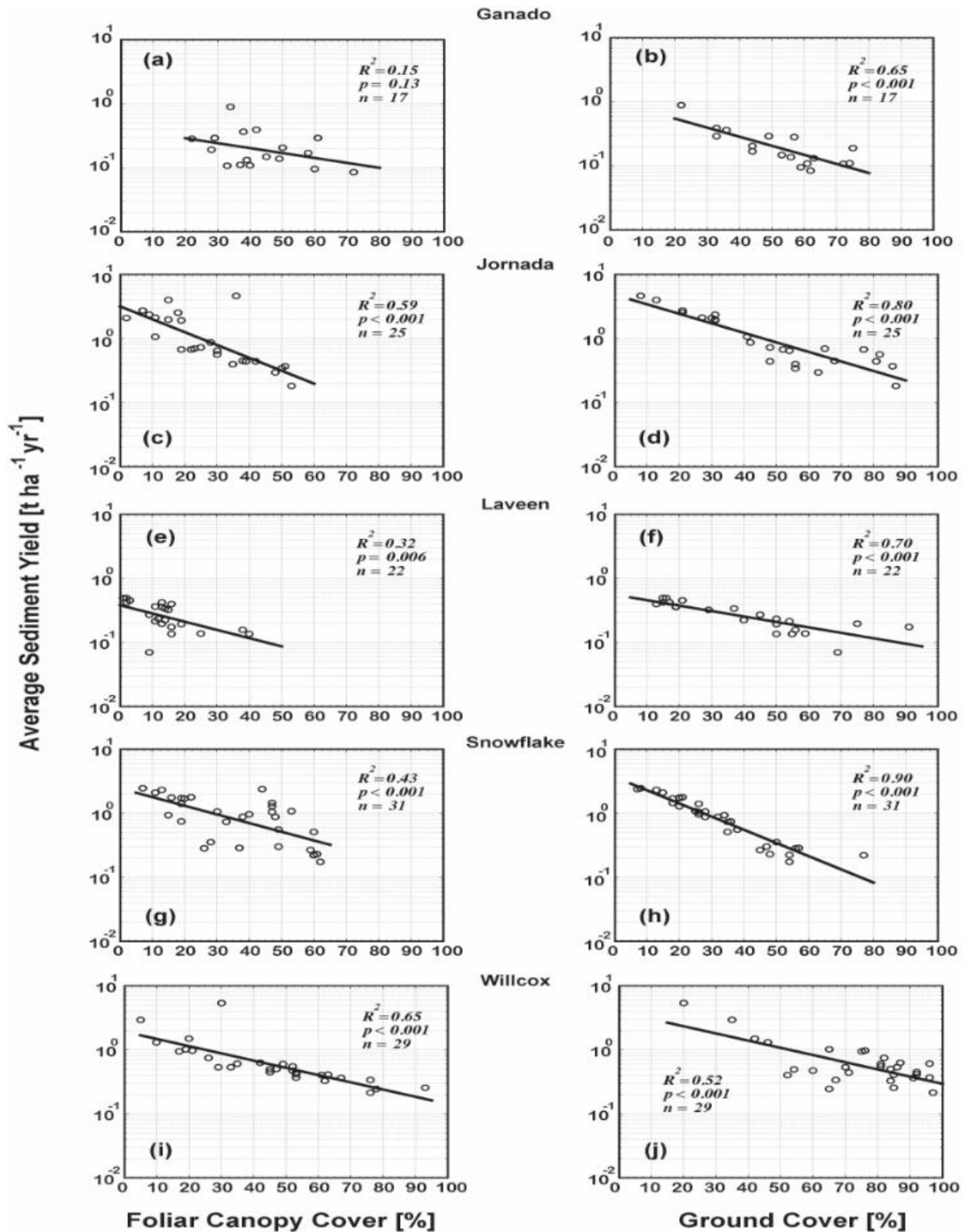
Figure 11. Association between predicted average sediment yield and foliar cover and ground cover for the five precipitation regimes.

References

Al-Hamdan O. Z, Pierson Jr., F. B., Nearing, M. A., Stone, J. J., Williams, C. J., Moffet, C. A., Kormos, P. R., Boll, J., Weltz, M. A. (2012a). Characteristics of concentrated flow hydraulics for rangeland ecosystems: Implications for hydrologic modeling. Earth Surface Processes and Landforms, 37:157–168.

Al-Hamdan, O. Z., Pierson, F. B., Nearing, M. A., Williams, C. J., Hernandez, M., Boll, J., Nouwakpo, S. K., Weltz, M. A., Spaeth, K. (2017). Developing a parameterization approach for soil erodibility for the rangeland hydrology and erosion model (RHEM). Transactions of the American Society of Agricultural and Biological Engineers, 60:85-94.

Al-Hamdan, O. Z., Pierson, F. B., Nearing, M. A., Williams, C. J., Stone, J. J., Kormos, P. R., Boll, J., Weltz, M. A. (2012b). Concentrated flow erodibility for physically based erosion models: Temporal variability in disturbed and undisturbed rangelands. Water Resources Research, 48:W07504.l.

Al-Hamdan, O. Z., Pierson, F. B., Nearing, M. A., Williams, C. J., Stone, J. J., Kormos, P. R., Boll, J., Weltz, M. A. (2013). Risk assessment of erosion from concentrated flow on rangelands using overland flow distribution and shear stress partitioning. Transactions of the American Society of Agricultural and Biological Engineers, 56:539-548.

Bennett, J. P. (1974). Concepts of mathematical modeling of sediment yield. Water Resources Research, 10:485-492.

Cerdà, A. (1998). Changes in overland flow and infiltration after a rangeland fire in a Mediterranean scrubland. Hydrological Processes, 12:1031-1042.

Davenport, D. W., Breshears, D. D., Wicox, B. P., Allen, C. D. (1998). Viewpoint: Sustainability of piñon-juniper ecosystems – a unifying perspective of soil erosion thresholds. Journal of Range Management, 51:231-240.

Dahlstrom, D. J. (2015). Calibration and uncertainty analysis for complex environmental models. Ground Water, 53:673-674.

Doherty, J. (1994). PEST: a unique computer program for model-independent parameter optimization. Water Down Under 94: Groundwater/Surface Hydrology Common Interest Papers; Preprints of Papers, 551.

Dortignac, E. J., Love, L. D. (1961). Infiltration studies on ponderosa pine ranges of Colorado. Infiltration studies on ponderosa pine ranges of Colorado.

Fair, G. M., Geyer, J. C. (1954). Water supply and wastewater disposal. In: Water supply and waste water disposal. John Wiley.

Foltz, R. B., Rhee, H., Elliot, W. J. (2008). Modeling changes in rill erodibility and critical shear stress on native surface roads. Hydrologic Processes, 22:4783-4788.

Foster, G. R. (1982). Modeling the erosion process. In: Hydrologic Modeling of Small Watersheds, Haan, C. T., Johnson, H. P., Brakensiek, D. L., (eds.). American Society of Agricultural Engineers Monograph, 5:297–360.

Gifford, G. F. (1985). Cover allocation in rangeland watershed management. In: Watershed Management in the Eighties. Jones, E. B., Ward, T. J., (eds.). American Society of Civil Engineers, 23–31.

Goebel, J. J. (1998). The national resources inventory and its role in U.S. agriculture, Agricultural Statistics 2000: An International Conference on Agricultural Statisticas, International Statistical Institute, 181-192.

Green, W. H., Ampt, G. A. (1911). Studies on soil physics, part I, the flow of air and water through soils. Journal of Agricultural Science, 4:11–24.

Gupta, H. V., Sorooshian, S., Yapo, P. O. (1999). Status of automatic calibration for hydrologic models: Comparison with multilevel expert calibration. Journal of Hydrologic Engineering, 4:135–143.

Havstad, K. M., Peters, D., B., Allen-Diaz, B., Bestelmeyer, B., Briske, D., Brown, J. R., Brunson, M., Herrick, J. E., Johnson, P., Joyce, L., Pieper, R., Svejcar, A. J., Yao, J., Bartolome, J., Huntsinger, L. (2009). The western United States rangelands, a major resource. In: Grassland, Quietness and Strength for a New American Agriculture, Chapter 5:75-93.

Hernandez, M., Nearing, M. A., Stone, J. J., Pierson, F. B., Wei, H., Spaeth, K. E., Heilman, P., Weltz, M. A., Goodrich, D. C. (2013). Application of a rangeland soil erosion model using National Resources Inventory data in southeastern Arizona. Journal of Soil and Water Conservation, 68:512-525.

Herrick, J. E., Wills, S., Karl, J., Pyke, D. (2010). Terrestrial indicators and measurements: Selection process and recommendations. U.S. Department of Agriculture.

Holland, M. E. (1969). Design and testing of rainfall system. Colorado State University Experimental Station, CER 69-70, MEH21, Fort Collins, Colorado.

Keefer, T. O., Renard, K. G., Goodrich, D. C., Heilman, P., Unkrich, C. L. (2015). Quantifying extreme rainfall events and their hydrologic response in southeastern Arizona. Journal of Hydrologic Engineering, 21:1-10.

Lane, L. J., Hernandez, M., Nichols, M. H. (1997). Dominant processes controlling sediment yield as functions of watershed scale. In: Proceedings of the International Conference on Modelling and Simulation, Hobart, Tasmania, McDonald, A.D., McAleer, M., (eds.). 1:5.

Ludwig, J. A., Wilcox, B. P., Breshears, D. D., Tongway, D. J., Imeson, A. C. (2005). Vegetation patches and runoff-erosion as interacting ecohydrological processes in semiarid landscapes. Ecology, 86:288–297.

Meeuwig, R. O. (1970). Infiltration and soil erosion as influenced by vegetation and soil in northern Utah. Journal of Range Management, 23:185-188.

Moffet, C. A., Pierson, F. B., Robichaud, P. R., Spaeth, K. E., Hardegree, S. P. (2007). Modeling soil erosion on steep sagebrush rangeland before and after prescribed fire. Catena, 71:218–228.

Moriasi, D. N., Arnold, J. G., Van Liew, M. W., Bingner, R. L., Harmel, R. D., Veith, T. L., (2007). Model evaluation guidelines for systematic quantification of accuracy in watershed simulations. Transactions of the American Society of Agricultural and Biological Engineers, 50:885–900.

Morris, S. E., Moses, T. A. (1987). Forest fire and the natural soil erosion regime in the Colorado Front Range. Annals of the Association of American Geographers, 77:245 – 254.

Nash, J. E., Sutcliffe, J. V. (1970). River flow forecasting through conceptual models part I - A discussion of principles. Journal of Hydrology, 10:282–290.

Nearing, M. A. (2000). Evaluating soil erosion models using measured plot data: Accounting for variability in the data. Earth Surface Processes and Landforms, 25:1035-1043.

Nearing, M. A., Hairsine, P. B. (2011). The Future of Soil Erosion Modelling. Ch. 20 In: Morgan, R. P., Nearing, M. A. (eds.). Wiley-Blackwell Publishers, Chichester, West Sussex, UK., 387-397.

Nearing, M. A., Jetten, V., Baffaut, C., Cerdan, O., Couturier, A., Hernandez, M., Le Bissonnais, Y., Nichols, M. H., Nunes, J. P., Renschler, C. S., Souchère, V., van Oost, K. (2005). Modeling response of soil erosion and runoff to changes in precipitation and cover. Catena, 61:131–154.

Nearing, M. A., Nichols, M. H., Stone, J. J., Renard, K. G., Simanton, J. R. (2007). Sediment yields from unit-source semiarid watersheds at Walnut Gulch. Water Resources Research 43:W06426.

Nearing M. A., Norton, L. D., Bulgakov, D. A., Larionov, G. A., West, L. T., Dontsova, K. M. (1997). Hydraulics and erosion in eroding rills. Water Resources Research, 33:865–876.

Nearing, M. A., Pruski, F. F., O'Neal, M. R. (2004). Expected climate change impacts on soil erosion rates: A review. Journal of Soil and Water Conservation, 59:43-50.

Nearing, M. A., Unkrich, C. L., Goodrich, D., Nichols, M. H., Keefer, T. O. (2015). Temporal and elevation trends in rainfall erosivity on a 149km^2 watershed in a semi-arid region of the American Southwest. International Soil and Water Conservation Research, 3:77–85.

Nearing, M. A., Wei, H., Stone, J. J., Pierson, F. B., Spaeth, K. E., Weltz, M. A., Flanagan, D. C., Hernandez, M. (2011). A rangeland hydrology and erosion model. Transactions of the American Society of Agricultural and Biological Engineers, 54:901-908.

Nichols, M. H., Nearing, M. A., Polyakov, V. O., Stone, J. J. (2012). A sediment budget for a small semiarid watershed in southeastern Arizona, USA. Geomorphology, 180-181:137-145.

Nicks, A. D., Lane, L. J., Gander, G. A. (1995). Weather generator. In: USDA-Water Erosion Prediction Project: Hillslope Profile and Watershed Model Documentation, Flanagan, D. C., Nearing, M. A. (eds.). NSERL Report 10:2-1.

Nielsen, D. R., Biggar, J. W., Erh, K. T. (1973). Spatial variability of field-measured soil-water properties. Hilgardia, 42:215-259.

Parlange, J. Y., Lisle, I., Braddock, R. D., Smith, R. E. (1982). The three-parameter infiltration equation. Soil Science, 133:337-341.

Peters, D. P. C., Bestelmeyer, B. T., Turner, M. G. (2007). Cross-scale interactions and changing pattern-process relationships: Consequences for system dynamics. Ecosystems, 10:790–796.

Petersen, S. L., Stringham, T. K., Roundy, B. A. (2009). A process-based application of state-and-transition models: A case study of western juniper (Juniperus occidentalis) encroachment. Rangeland Ecology & Management, 62:186–192.

Pierson, F. B., Bates, J. D., Svejcar, T. J., Hardegree, S. P. (2007). Runoff and erosion after cutting western juniper, Rangeland Ecology & Management, 60:285–292.

Pierson, F. B., Carlson, D. H., Spaeth, K. E. (2002). Impacts of wildfire on soil hydrological properties of steep sagebrush-steppe rangeland. International Journal of Wildland Fire, 11:145 – 151.

Pierson, F. B., Moffet, C. A., Williams, C. J., Hardegree, S. P., Clark, P. E. (2009). Prescribed-fire effects on rill and interrill runoff and erosion in a mountainous sagebrush landscape. Earth Surface Processes and Landforms, 34:193–203.

Pierson, F. B., Robichaud, P. R., Moffet, C. A., Spaeth, K. E., Hardegree, S. P., Clark, P. E., Williams, C. J. (2008). Fire effects on rangeland hydrology and erosion in a steep sagebrush-dominated landscape. Hydrological Processes, 22:2916–2929.

Pierson, F. B., Williams, C. J., Hardegree, S. P., Clark, P. E., Kormos, P. R., Al-Hamdan, O. Z. (2013). Hydrologic and erosion responses of sagebrush steppe following juniper encroachment, wildfire, and tree cutting. Rangeland Ecology & Management, 66:274–289.

Pierson, F. B., Williams, C. J., Kormos, P. R., Hardegree, S. P., Clark, P. E., Rau, B. M. (2010). Hydrologic vulnerability of sagebrush steppe following pinyon and juniper encroachment. Rangeland Ecology & Management, 63:614–629.

Rawls, W. J., Brakensiek, D. L., Saxton, K. E. (1982). Estimation of soil water properties. Transactions of the American Society of Agricultural and Biological Engineers, 81-2510.

Rawls, W. J., Brakensiek, D. L., Simanton, J. R., Kho, K. D. (1990). Development of a crust factor for a Green Ampt model. Transactions of the American Society of Agricultural and Biological Engineers, 33:1224-1228.

Rawls, W. J., Gimenez, D., Grossman, R. (1998). Use of soil texture, bulk density, and slope of the water retention curve to predict saturated hydraulic conductivity. Transactions of the American Society of Agricultural and Biological Engineers, 41:983-988.

Renard, K. G. (1980). Estimating erosion and sediment yield from rangeland. In: Proceedings of ASCE Symposium on Watershed Management, Boise, ID, 164-175.

Robichaud, P. R., Ashmun, L. E., Sims, B. D. (2010). Post-fire treatment effectiveness for hillslope stabilization. US Department of Agriculture, Forest Service, Rocky Mountain Research Station, General Technical Report RMRSGTR-240. DIANE Publishing.

Sala, O. E., Lauenroth, W. K., Parton, W. J., & Trlica, M. J. (1981). Water status of soil and vegetation in a shortgrass steppe. Oecologia, 48(3), 327-331.

Scott, D. F., van Wyk, D. B. (1992). The effects of fire on soil water repellency, catchment sediment yields and stream flow. In: Fire in South African Mountains Fynbos. Springer Berlin Heidelberg, 93:216-239.

Shakesby, R. A., Coelho, C. D. A., Ferreira, A. D., Terry, J. P., Walsh, R. P. D. (1993). Wildfire impacts on soil-erosion and hydrology in wet Mediterranean Forest, Portugal. International Journal of Wildland Fire, 3:95-110.

Simanton, J. R., Osterkamp, W. R., Renard, K. G. (1993). Sediment yield in a semiarid basin: Sampling equipment impacts. IAHS publication, 3-3.

Smith, R. E., Corradini, C., Melone, F. (1993). Modeling infiltration for multi-storm runoff event. Water Resources Research, 29:133-44.

Smith, R. E., Goodrich, D. C. (2000). Model for rainfall excess patterns on randomly heterogeneous areas. Journal of Hydrology Engineering, 5:355–362.

Smith, R. E., Goodrich, D. C., Woolhiser, D. A., Unkrich, C. L. (1995). KINEROS - a kinematic runoff and erosion model. In: Computer Models of Watershed Hydrology, V.P. Singh (eds.). Water Resources Publications, 20:697-732.

Smith, R. E., Parlange, J. Y. (1978). A parameter-efficient hydrologic infiltration model. Water Resources Research, 14:533-538.

Spaeth, K. E., Pierson, F. B., Weltz, M. A., Awang, J. B. (1996). Gradient analysis of infiltration and environmental variables as related to rangeland vegetation. Transactions of the American Society of Agricultural and Biological Engineers, 39:67-77.

Stone, J. J., Lane, L. J., Shirley, E. D. (1992). Infiltration and runoff simulation on a plane. Transactions of the American Society of Agricultural and Biological Engineers, 35:161-170.

Swanson, N. P. (1965). Rotating–boom rainfall simulator. Transactions of the American Society of Agricultural and Biological Engineers, 8:71–72.

Thompson, S. E., Harman, C. J., Heine, P., Katul, G. G. (2010). Vegetation-infiltration relationships across climatic and soil type gradient. Journal of Geophysical Research, 115:G02023.

Tromble, J. M., Renard, K. G., Thatcher, A. P. (1974). Infiltration for three rangeland soil-vegetation complexes. Journal of Range Management, 27:318-321.

Turnbull, L., Wainwright, J., Brazier, R. E. (2008). A conceptual framework for understanding semi-arid land degradation: Ecohydrological interactions across multiple-space and time scales. Ecohydrology, 1:23–34.

Turnbull, L., Wilcox, B. P., Belnap, J., Ravi, S., D'Odorico, P., Childers, D., Gwenzi, W., Okin, G., Wainwright, J., Caylor, K. K., Sankey, T. (2012). Understanding the role of ecohydrological feedbacks in ecosystem state change in drylands. Ecohydrology, 5:174–183.

Urgeghe, A., Breshears, D., Martens, S., & Beeson, P. (2010). Redistribution of Runoff Among Vegetation Patch Types: On Ecohydrological Optimality of Herbaceous Capture of Run-On. Rangeland Ecology & Management, 63(5), 497-504.

Urgeghe, A. M., & Bautista, S. (2015). Size and connectivity of upslope runoff-source areas modulate the performance of woody plants in Mediterranean drylands. Ecohydrology, 8(7), 1292-1303. doi:10.1002/eco.1582

UNCCD. (1994). United Nations convention to combat desertification in countries experiencing serious drought and/or desertification, particularly in Africa. Homepage UNCCD: www.unccd.int.

Wainwright, J., Parsons, A. J., Abrahams, A. D. (2000). Plot-scale studies of vegetation, overland flow and erosion interactions: Case studies from Arizona and New Mexico. Hydrological Processes, 14:2921–2943.

Wei, H., Nearing, M. A., Stone, J. J., Guertin, D. P., Spaeth, K. E., Pierson, F. B., Nichols, M. H., Moffett, C. A. (2009). A new splash and sheet erosion equation for rangelands. Soil Science Society of America Journal, 73:1386-1392.

Weltz, M. A., Kidwell, M. R., Fox, H. D. (1998). Influence of abiotic and biotic factors in measuring and modeling soil erosion on rangelands: State of knowledge. Journal of Range Management, 51:482-495.

Weltz, M. A., Speath, K. E., Taylor, M. H., Rollins, K., Pierson, F. B., Jolley, L. W., Nearing, M. A., Goodrich, D. C., Hernandez, M., Nouywakpo, S., Rossi, C. (2014). Cheatgrass invasion and woody species encroachment in the Great Basin: Benefits of conservation. Journal of Soil and Water Conservation, 69:39A-44A.

Wilcox, B. P. (1994). Runoff and erosion in intercanopy zones of pinyon-juniper woodlands. Journal of Range Management, 285-295.

Wilcox, B. P., Breshears, D. D., & Allen, C. D. (2003). Ecohydrology of a resource-conserving semiarid woodland: Effects of scale and disturbance. Ecological Monographs, 73(2), 223-239.

Wilcox, B. P., Seyfried, M. S., Breshears, D. D., McDonnell, J. J. (2012). Ecohydrologic connections and complexities in drylands: New perspectives for understanding transformative landscape change. Ecohydrology, 5:143–144.

Williams, C. J., Pierson, F. B., Robichaud, P. R., Boll, J. (2014). Hydrologic and erosion responses to wildfire along the rangeland–xeric forest continuum in the western US: A review and model of hydrologic vulnerability. International Journal of Wildland Fire, 23:155-172.

Williams, C. J., Pierson, F. B., Spaeth, K. E., Brown, J. R., Al-Hamdan, O. Z., Weltz, M. A., Nearing, M. A., Herrick, J. E., Boll, J., Robichaud, P. R., Goodrich, D. C., Heilman, P., Guertin, D. P., Hernandez, M., Wei, H., Hardegree, S. P., Strand, E. K., Bates, J. D., Metz, L. J., Nichols, M. H. (2016). Incorporating hydrologic data and ecohydrologic relationships into ecological site descriptions. Rangeland Ecology & Management, 69:4-19.

Woolhiser, D. A., Smith, R. E., Goodrich, D. C. (1990). KINEROS, a kinematic runoff and erosion model: Documentation and user manual. U. S. Department of Agriculture, Agricultural Research Service, p. 5.

Zhang, X. C., Nearing, M. A., Risse, L. M. (1995). Estimation of green-ampt conductivity parameters: Part I. row crops. Transactions of the American Society of Agricultural and Biological Engineers, 38:1069-1077.

Appendix I. Conversion Factors

Multiply	By	To obtain
degree Celsius (°C)	33.8	degree Fahrenheit (°F)
millimeter (mm)	3.94×10^{-2}	inch (in)
centimeter (cm)	3.94×10^{-1}	inch (in)
meter (m)	3.28	feet (ft)
kilometer (km)	6.21×10^{-1}	mile (mi)
gram (g)	3.53×10^{-2}	ounce (oz)
kilogram (kg)	2.205	pound (lb)
square meter (m^2)	10.76	square foot (ft^2)
square meter (m^2)	2.47×10^{-4}	acre (ac)
hectare (ha)	2.47	acre (ac)
square kilometer (km^2)	3.86×10^{-1}	square mile (mi^2)
square kilometer (km^2)	247	acre (ac)
cubic meter (m^3)	35.3	cubic foot (ft^3)
liter (L)	3.53×10^{-2}	cubic foot (ft^3)
millimeter per hour (mm h^{-1})	3.94×10^{-2}	inch per hour (in h^{-1})
liter per second (L s^{-1})	3.53×10^{-2}	cubic foot per second (ft^3 s^{-1})
cubic meter per second (m^3 s^{-1})	35.3	cubic foot per second (ft^3 s^{-1})
gram per square meter (g m^{-2})	4.46×10^{-3}	ton per acre (t ac^{-1})
kilogram per hectare (kg ha^{-1})	4.46×10^{-4}	ton per acre (t ac^{-1})
megagram (Mg)	1.102	ton (t)

Appendix II. Vegetation and ground cover definitions and photograhs

Biological Soil Crust

Biological Soil Crust

Salt Crusts and Biological Soil Crust

Micro Shrub Coppice Dune and Bare Soil

Sod Grass with Bare Interspace

Sod Grass with Manure and Litter

Rock, Bare Interspace and Trace Litter

Rock, Bare Interspace and Trace Litter

Shrub with Forbs in Foreground

Bunchgrass with Woody Agave

Litter and Bare Soil

Bunchgrass, Annual Grass, Rock, Litter & Bare Soil

Juniper Trees Invading Bunchgrass

Savanna with Tallgrass and Scattered Trees

Shrubland with Open Interspace and Encroachment by Juniper Trees

Shrubland with Bunchgrass Interspace

Shrub, Rock and Bare Soil

Shrub, Cacti, Rock and Bares Soil

Forb in Bunchgrass

Forb in Bunchgrass

Forb

Forb in Litter

Wind Erosion Showing bare soil and burned basal stumps of shrubs

Forbs in mixed grass Prairie

Hydrologic Terms

Raindrop Splash Erosion

Sheet Flow Erosion

Concentrated Flow Path/Rill

Concentrated Flow Path/Rill

Flash Flood/Stream Flow

Gully Erosion